Ultraviolet photoinduced weak bonds in aryl-substituted polysilanes

2007 J. Phys.: Condens. Matter 19 076101

(http://iopscience.iop.org/0953-8984/19/7/076101)

INSTITUTE OF PHYSICS PUBLISHING JOURNAL OF PHYSICS: CONDENSED MATTER

J. Phys.: Condens. Matter **19** (2007) 076101 (11pp) doi:10.1088/0953-8984/19/7/076101

Ultraviolet photoinduced weak bonds in aryl-substituted polysilanes

F Schauer[1], I Kuřitka[1], P Sáha[1] and S Nešpůrek[2]

[1] Polymer Centre, Tomas Bata University in Zlin, Faculty of Technology, T G Masaryka 275, CZ 762 72 Zlin, Czech Republic
[2] Institute of Macromolecular Chemistry, Academy of Sciences of the Czech Republic, 162 06 Prague, Czech Republic

Received 3 April 2006, in final form 10 November 2006
Published 15 January 2007
Online at stacks.iop.org/JPhysCM/19/076101

Abstract

The susceptibility of aryl-substituted polysilylenes to photodegradation by ultraviolet (UV) radiation is examined on the prototypical materials poly[methyl(phenyl)silylene] (PMPSi) and poly[(biphenyl-4-yl)methylsilylene] (PBMSi). We extend the scope of our last paper (Schauer *et al* 2004 *Polym. Degrad. Stabil.* **84** 383) with the elucidation of the degradation mechanisms for two different degradation wavelengths: 266 and 355 nm. The main purpose of this paper was to study photoluminescence (PL) after major degradation, predominantly in long-wavelength range 400–600 nm, studying the disorder, dangling bonds (DBs) and weak bonds (WBs) created by the degradation process. We claim that the PL of the 500–600 nm band is related to the existence of WBs on the Si chain and originates in the σ^*–σ exciton migration at room temperature by diffusion, free electron–hole formation, trapping in WBs and subsequent radiative recombination by tunnelling. Increase of the normalized PL 520–540 nm band after UV degradation can be then evaluated as the increase of the density of states (DOS) of WBs. The efficiency of the WB creation in PMPSi is greater for 266 nm irradiation, supporting the notion of the suppressed exciton transport compared to the less energetical photon of 355 nm, where the WB creation is lowered due to the exciton migration to longer segments and/or already existing defects. For PBMSi the WB creation kinetics for 355 nm degradation is similar to that of PMPSi. The 266 nm degradation results then support the model calculations of DB and WB reconstruction in the more rigid Si skeleton.

1. Introduction

High molecular weight silicon backbone polymers, polysilanes (PSs), currently constitute a topical research field due to a wide spectrum of optoelectronic applications, namely because of their unique nonlinear optical, photostructural and photoelectronic properties [1–3]. Besides,

photostructural, degradation and metastable changes make PSs promising materials for future resists for nanostructural fabrication [4].

Thin film solid-state polysilanes are glassy materials with the random chain model as the widely accepted structural model, with flexible (underconstrained) bonding structure, prototypical in studies of the structural dimensionality of their properties, with the typical quality of identical properties with the only differences depending on the preparation techniques. The defect structure of polysilanes is formed by intrinsic defects that are deviations from the optimally bonded network and conformation; the most common defects will be those with the smallest free energy of creation [5].

The physical properties of polysilylenes are strongly influenced by the chemical structure of side groups. The absorption spectrum of a solid film of a typical polysilylene, poly[methyl(phenyl)silylene] (PMPSi), consists of three main peaks with maxima at 332 nm (absorption coefficient $\alpha = 1.55 \times 10^5$ cm^{-1}), 270 nm ($\alpha = 1.16 \times 10^5$ cm^{-1}) and 194 nm ($\alpha = 5.43 \times 10^5$ cm^{-1}) [6]. It has been shown that the first long-wavelength electronic transition arises mainly from delocalized σ–σ^* transitions, the contribution of π–π^* transitions to the longest-wavelength band is weak [7]. It was found that with increasing aromaticity of the side substituents the character of the first (σ–σ^*) optical transition (Si–Si excitation in PMPSi) changed more to the π–π^* type of transition, e.g. in poly[(biphenyl-4-yl)methylsilylene] (PBMSi). The peak at $\lambda = 270$ nm is associated with π–π^* transitions in the benzene ring. In addition to the σ–σ^* and π–π^* types of absorption band, a very weak tail in the visible region was observed [8]. The band theory calculations [9, 10] suggested that the first allowed optical transition at 3.5–4.0 eV resulted from a band-to-band transition in PMPSi. The lowering of the band gap energy E_g in comparison with the value of 4.5 eV for poly(dialkylsilylene)s was ascribed to a (σ, π) band mixing at the valence band edge state [11] between the skeleton Si 3p and π HOMO states of benzene rings as side chain substituents.

In the luminescence spectra, only the σ^*–σ transitions situated at 356 nm participate, due to the very fast non-radiative transitions π^*–σ^*. The observed visible photoluminescence situated in both PMPSi and PBMSi in a broad band 400–600 nm is described in detail in section 3.

Glassy materials exhibit metastability. Very pronounced changes in their physical, chemical or structural properties are observed when exposed to UV radiation. These photoinduced changes may be either irreversible or reversible by thermal annealing to the glass transition temperature T_g. Thus, the mechanism for photostructural changes and/or concomitant metastability is of fundamental importance. Basically they may be manifested in for example polysilanes as Si–Si bond scission, forming dangling bonds (DBs), or as the creation of strained Si–Si bonds, called weak bonds (WBs). They were studied by electron-spin resonance [12] and both steady-state and transient photoconductivity [13, 14]. There is a generally accepted model for the DB formation and its reconstruction. The observation of progressive blue shift in the maximum of the σ–σ^* absorption suggests that the polymer molecular weight is reduced by UV radiation [15], in a way that is very similar to photoinduced changes in amorphous hydrogenated silicon (a-Si:H) [16] and photodarkening effects observed in chalcogenide glasses [17]. Naito [18] also found two types of DB in PSs and describes their annealing behaviour by a two-well potential configurational diagram.

On the other hand, the metastability issue, especially that connected with WBs, is far less studied, though it seems to possess unique properties in PSs as it is related to the conformational transformations. This topic is of prime importance for optical and electronic applications of any glassy semiconductor as the electronic properties of such materials are strongly connected with the electronic structure and this, in turn, is decisive for density of (electron localized) states (DOS) distribution. Such localized states are one of the most basic characteristics of amorphous semiconductors with respect to applications in optoelectronic devices. Despite

decades of research, the problem of the DOS in polysilanes still remains controversial. It was also experimentally proved that the increased WB concentration increases the disorder [19].

The WB formation was first theoretically addressed using first-principles electronic calculations. Takeda *et al* in [12] found the WB to act as a self-trapping centre for the σ^* state that may be easily scissored as a result of an interaction with the surrounding medium. Due to differences in the local atomic configurations a wide spread of activation energies was predicted [20] and used for PL degradation kinetics modelling [21]. Two types of photocreated metastable state, one for the low photoexcitation energy (∼3.5 eV) due to the Si skeleton stretching forces and the other for the higher photoexcitation energy (∼4.8 eV) related to the formation of WBs, as bonds of inferior quality, were found by light-induced ESR and model calculations [12] and explained by optically selective scissoring. The WB is considered by stretching a part of the uniform Si skeleton bond. As a result, the local Si skeleton bond stretching weakens the pσ bonding character and the highest occupied valence band (HOVB) state and destabilizes it. Therefore, the original HOVB state shifts energetically upwards and forms a hole-tail state with localization around the WB site. Conversely, a reduction in the spσ^* antibonding character stabilizes the lowest unoccupied conduction band (LUCB) state energetically to shift the original LUCB state downwards, and an electron-tail state is formed. Fujiki [22] found a correlation of NMR signals occurring on introduction of branching points with the defect luminescence at 450 nm at a level in excess of 1% of such bonding configurations. His explanation was based on the formation of organosilane units with lengthened (strained) Si–Si weak bonds leading to the band tails in the electron structure of the valence highest occupied molecular orbital (HOMO) and the conduction lowest unoccupied molecular orbital (LUMO) bands. Nakayama, in a series of papers [21, 23], presented a detailed model for absorption and photoluminescence changes, based on DB creation with WBs possessing a wide distribution of activation energies as a precursor for DB creation. The time of flight technique was used by Naito [24], who found that the degradation by UV radiation creates DBs and WBs, which do not influence the drift mobility of charge carriers, but create the disorder. The annealing restores the collection efficiency of the holes, but does not affect the disorder, concluding that the disorder was caused by the conformational changes.

Transient photoconductivity and post-transit photoconductivity [13, 14] were used to study the electron structure of the products of photodegradation of poly[methyl(phenyl)silylene] (PMPSi) and also the metastability issue. We found that the bond cleavage or weakening resulted in the formation of deep electronic states of differing parameters (energy positions and capture cross-sections), depending on the presence or absence of oxygen. In vacuum or in inert atmosphere, the weakened bonds constitute deep electronic states situated 0.45–0.55 eV above the HOMO level depending on the energy of the excitation. It was found by measuring the photoluminescence [25] that metastable electronic states are 0.45 eV deep, and that the scissoring energy depends on photodegradation wavelength (250–280 and 366 nm). These metastable states are amenable to annealing with activation energy of 0.65 eV. The existence of the radiation-driven metastability and thermally driven recovery of Si–Si bonds was also found by the method of thermally stimulated luminescence. It was supposed that in PSs there is an energy transfer to the longest segments and that photochemical events occur in these segments. The scission of Si–Si bond and the transfer of the excitation to the longest segments are competitive processes. In [27] there is described the degradation of poly(di-*n*-hexyl-silylene) (PDHS) and PMPS; there was found a decisive difference for the degradation at 265 and 365 nm: in the former case the cutting of the Si–Si bonds occurred not selectively (not shifting the absorption peak) and in the latter case it did occur selectively, cutting the longest segments (and those with defects), thus shifting the exciton absorption to shorter wavelength (testifying the remaining shorter segments).

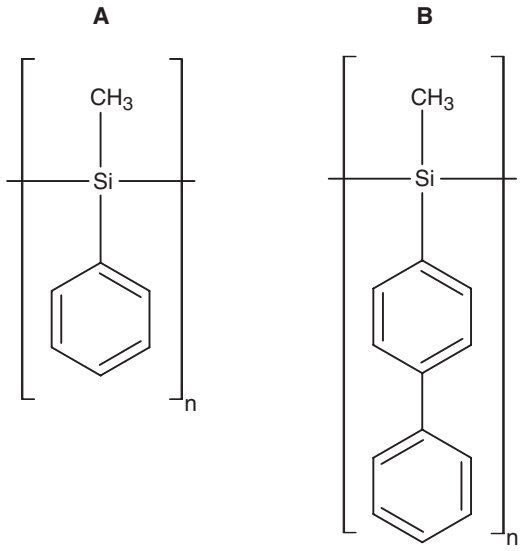

Scheme 1. Synthesized polymers used in this study. (A) poly[methyl(phenyl)silylene], (B) poly[biphenyl-4-yl(methyl)silylene].

A decisive experiment on the influence of conformational changes on the fluorescence in poly(di-n-hexylsilane) was presented recently [28]; nanosized polysilane was introduced into mesoporous silica and 420 nm fluorescence was observed in 2.8 nm pores.

This paper is the continuation of our first paper [29], in which we used identical materials represented by the aryl-substituted polysilanes poly[methyl(phenyl)silylene] (PMPSi) and poly[(biphenyl-4-yl)methylsilylene] (PBMSi) (see scheme 1) for the degradation experiments. We extend the scope of the first paper with the elucidation of the degradation mechanisms for two different degradation wavelengths of radiation, 266 and 355 nm. The main purpose of this paper was to study PL after major degradations, predominantly in the long-wavelength range 400–600 nm, studying the disorder and WBs created by the degradation process.

2. Experimental details

The experimental details concerning the preparation of PSs are given in detail in our previous paper [29]. Films for photoluminescence measurements were prepared from a toluene solution by spin coating (2000 rpm, 50 s) on glass and single-crystal silicon substrates. The thickness of the films was about 500 nm. For IR absorption measurements, Nicolet 400 FTIR and FT-IR microscope Continuum Nicolet were used. The Nd:YAG laser Continuum Minilite II (Electro-Optics) was used for excitation and a CCD camera Oriel (model DB 401-UV) scanned emission spectra. This set-up was used both to pick up PL spectra excited by the available laser wavelengths (266 and 355 nm) and to study the UV degradation of the materials examined.

3. Experimental results

The degradation kinetics and mechanisms differ with respect to both degradation wavelengths and chemical composition of the materials used. We want to demonstrate this fact on aryl-substituted PMPSi and PBMSi.

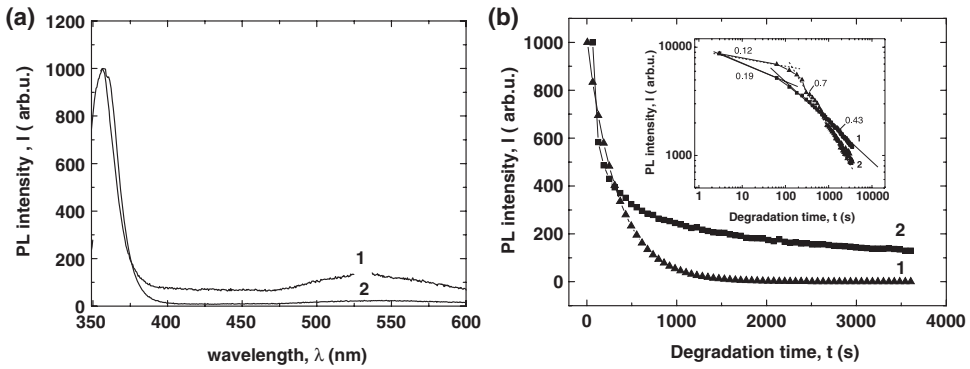

Figure 1. (a) Room-temperature photoluminescence emission spectra of PMPSi; the normalized PL excitation spectra of the virgin PMPSi for two excitation wavelengths, 266 nm (curve 1) and 355 nm (curve 2); (b) time decay of PL emission intensity at $\lambda = 356 \pm 5$ nm during the photodegradation by $\lambda_{deg} = 266$ nm (curve 1) and $\lambda_{deg} = 355$ nm (curve 2).

PMPSi

Figure 1(a) shows the normalized PL excitation spectra of the virgin PMPSi for two excitation wavelengths, 266 and 355 nm. In both cases the exciton bands, situated at 356 ± 5 nm, and very weak PL bands at ≈420 nm and ≈540 nm are visible, in accordance with [30]. During degradation, the excitonic PL band decreases with the photodegradation time: the degradation time dependences of the intensity of the excitonic PL measured at 356 ± 5 nm for the degradation and excitation wavelengths 266 and 355 nm are given in figure 1(b). The kinetics of the degradation are similar, consisting of the region with $I \sim t^{-n}$ for $t < t_T$ and the region with $I \sim t^{-m}$, where t_T is the transition time between these two regions. In case of 266 nm degradation wavelength the kinetics of degradation gives $n = 0.12$ and $m = 0.70$ and $t_T = 145$ s, whereas for 355 nm degradation $n = 0.19$, $m = 0.43$ and $t_T = 90$ s.

Figure 2(a) shows the PL spectra taken after 1 h degradation at degradation wavelengths 266 and 355 nm at room temperature, normalized for the PL intensity of the σ^*–σ exciton band at 356 ± 5 nm. The most striking result is the progressive increase of the band at 540 nm after 1 h degradation, as is obvious from comparison with figure 1(a). Whereas the 355 nm degradation changed the band at 540 nm very little, the 266 nm degradation increased both the PL bands at ≈420 nm and especially the 540 nm band. The kinetics of the increase of the 540 nm band with degradation time for both degradation wavelengths 266 and 355 nm are given in figure 2(b), in both linear and logarithmic coordinates. The PL band at 540 nm increases with progressive degradation, though with different efficiency and kinetics, as is visible from the inset, where the band normalized PL increases as $I_{540\ nm} \approx t^{1/2}$ and $I_{540\ nm} \approx t^{1/3}$ for 266 and 355 nm, respectively. The created states are metastable and are annealed even at room temperature. Figure 3 shows the evolution of the 540 nm PL band created by 266 nm degradation after two days at room temperature.

PBMSi

Figure 4(a) shows the normalized PL excitation spectra of the virgin PBMSi for two excitation wavelengths: 266 and 355 nm. In both cases the exciton bands, situated at 370 ± 5 nm, are visible and also very expressed bands at ≈420 and ≈500 nm. During degradation, the excitonic PL band decreases with the photodegradation time; the degradation time dependences

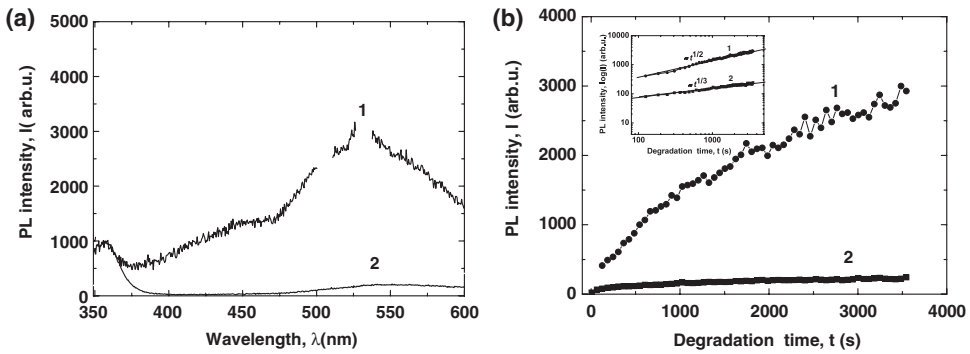

Figure 2. (a) PL emission spectra of PMPSi film after 60 min photodegradation by radiation of $\lambda_{deg} = 266$ nm (curve 1) and $\lambda_{deg} = 355$ nm (curve 2); (b) time evolution in PL emission intensity of the 540 nm band during photodegradation by $\lambda_{deg} = 266$ nm (curve 1) and $\lambda_{deg} = 355$ nm (curve 2).

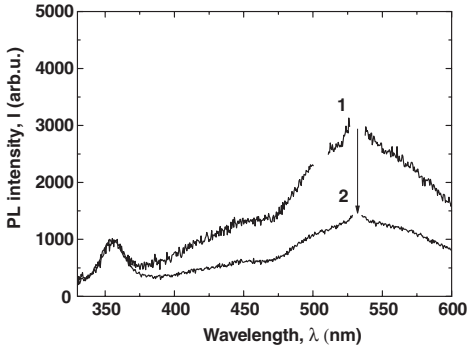

Figure 3. Time evolution of the PL emission spectra of PMPSi film after 60 min photodegradation by radiation with $\lambda_{deg} = 266$ nm (curve 1); after two days of relaxation at room temperature (curve 2).

of the intensity of the excitonic PL measured at 370 ± 5 nm for the degradation and excitation wavelengths 266 and 355 nm are given in figure 4(b). A considerably different and wavelength-dependent degradation kinetics is obvious. The kinetics of the degradation of the excitonic PL band observed after the degradation and excitation at 355 nm is similar to that of PMPSi from figure 1(b), $I \sim t^{-n}$ for $t < t_T$ and the region with $I \sim t^{-m}$. In case of 266 nm degradation, the kinetics of degradation dependence gives $n = 0.13$ for $t < t_T$ and $m = 0.5$ for $t > t_T$, where $t_T = 80$ s. The degradation of the excitonic PL band observed after the degradation and excitation at 266 nm exhibits quite different kinetics, described already in our previous paper [29] showing similar PL time decrease in the initial phase of irradiation, but then showing an increase and tending towards saturation (figure 4(b)). Figure 5(a) shows the PL spectra taken after 1 h degradation by degradation radiation wavelengths 266 and 355 nm at room temperature, normalized to the PL intensity of the exciton band at 370 ± 5 nm. The increase of both PL bands at $\lambda \approx 420$ and $\lambda \approx 500$ nm compared with the results given in figure 4(a) is obvious, without any change of the shape of the PL spectra. The kinetics of the increase of the 500 nm band with degradation time for both degradation wavelengths 266 and 355 nm are shown in figure 5(b), in both linear and logarithmic coordinates. The PL band at 500 nm increases with progressive degradation, though with substantially different

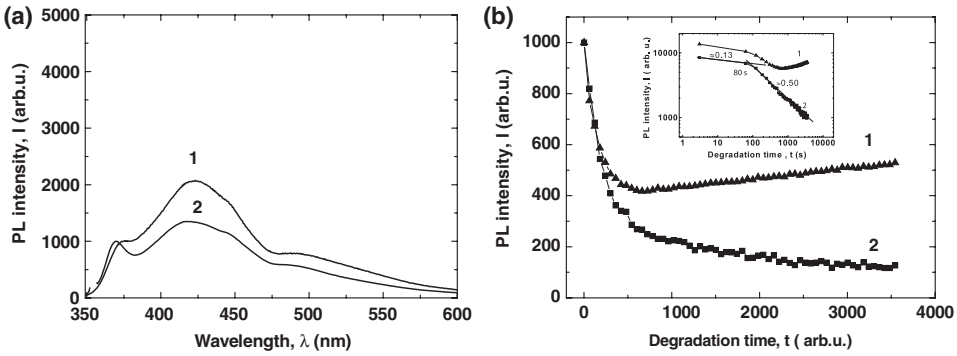

Figure 4. (a) Room-temperature photoluminescence emission spectra of PBMSi after photodegradation by radiation with $\lambda_{deg} = 266$ nm (curve 1) and $\lambda_{deg} = 355$ nm (curve 2); (b) time decrease in PL emission intensity at 370 ± 5 nm during photodegradation by radiation with $\lambda_{deg} = 266$ nm (curve 1) and $\lambda_{deg} = 355$ nm (curve 2).

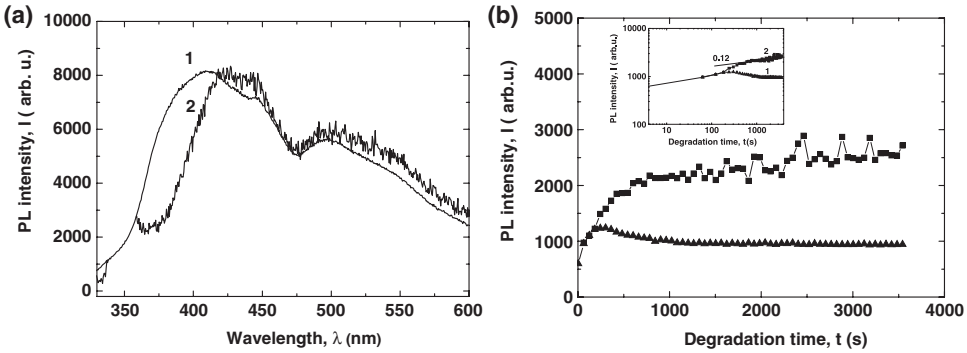

Figure 5. (a) PL emission spectra of PBMSi film after 60 min photodegradation by radiation with $\lambda_{deg} = 266$ nm (curve 1) and $\lambda_{deg} = 355$ nm (curve 2); (b) time evolution in PL emission intensity of the 500 nm band during photodegradation by radiation with $\lambda_{deg} = 266$ nm (curve 1) and $\lambda_{deg} = 355$ nm (curve 2).

kinetics, as is visible from the inset. The increase of the 500 nm PL band after degradation with radiation of $\lambda = 355$ nm follows $I_{500\,nm} \approx t^{1/8}$ dependence, whereas the degradation with 266 nm increases the PL in the same manner as at 266 nm, but then gives a maximum after which saturation is observed. The created states are metastable and are annealed even at room temperature. Figure 6 shows the evolution of the PL spectra of PBMSi created by 355 nm degradation and subsequent anneal.

4. Discussion and conclusions

In discussing the experimental results, let us concentrate on several firmly established facts. WBs are the primary consequence of the glassy state and/or external field excitation of any glassy solid-state material in general and in polysilanes in particular [5]. According to calculations, the DBs and/or WBs in polysilanes are created selectively depending on the wavelength of the radiation [12]. As both electrons and holes in WBs maintain their original orbital symmetries, an optical transition between them is possible, so a WB acts as a radiative centre with a strong PL; a DB, on the other hand, is non-radiative centre, suppressing PL.

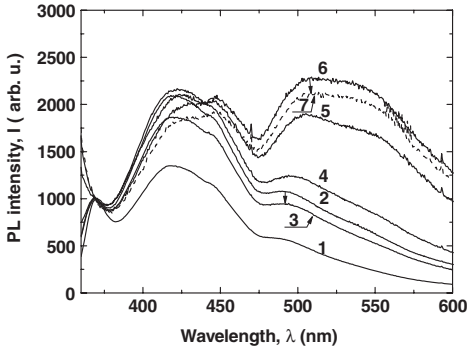

Figure 6. Evolution of the PL emission spectra of PBMSi film; pristine film (curve 1), after 5 min photodegradation by radiation with $\lambda_{deg} = 355$ nm (curve 2); after 1 h relaxation at 85 °C (curve 3); after another 5 min photodegradation by radiation with $\lambda_{deg} = 355$ nm (curve 4); after another 60 min photodegradation with $\lambda_{deg} = 355$ nm (curve 5); after 3 h relaxation at 85 °C and 2 h slow cooling (curve 6); after 12 h rest (curve 7).

The PL in polysilanes has been a much-disputed problem. Whereas much is known about the excitonic PL band due to the σ^*–σ deexcitation of the Si–Si chain in the 350–400 nm range, the energy transfer and the mechanism of Si–Si cutting causing degradation [31], little is known about the PL in the visible range 400–600 nm. Two possible explanations have been suggested, the first one based on the σ, π^* charge transfer (CT) model [12, 32] and the second on the backbone defect model [22, 33–36]. Molecular orbital calculations of the polymer chain at the branching points of the polysilane dendrimers give rise to the change of bond angle at the branching point, causing the defect. In [22] the authors found a correlation of NMR signals occurring on the introduction of branching points with defect luminescence at 450 nm [37] at a level in excess of 1% of such bonding configurations. Their explanation was based on the formation of organosilane units with lengthened (strained) Si–Si weak bonds leading to the band tails in the electron structure of the valence (HOMO) and conduction (LUMO) bands. The broad emission originates from the trapping site following an extreme energy migration [38]. The PL emission maximum of the broad band shifts gradually to longer wavelengths with increasing branching of the structure—this may be due to a lowering of the energy level of the trapping site. A decisive experiment concerning the influence of the conformational changes on the fluorescence in poly(di-n-hexylsilylene) was presented recently [28]; nanosized polysilane was introduced into mesoporous silica and 420 nm fluorescence was observed using 2.8 nm pores, whereas this was not observed in 5.8 nm pores and on homogeneous silica substrate, a fact explained by the existence of distortion-related localized states, where host–guest interactions substantially affect the conformation of the polymer chain. The conformation changes, in turn, induce localized excited states resulting in the emergence of a new band in the PL spectrum situated at 420 nm.

The PL spectra shown in figures 1(a) and 4(a) for PMPSi and PBMSi exhibit typical excitonic PL bands σ^*–σ transitions situated at 365 ± 5 and 370 ± 5 nm, respectively, and the long-wavelength, 'visible' PL bands located at 400–420 and 500–600 nm [30]. The much more expressed 400 and 500 nm PL bands in PBMSi support the notion that PBMSi is a much more disordered material compared to PMPSi due to the bulkiness and rigidity of the biphenyl groups.

The corresponding degradation kinetics are shown in figures 1(b) and 4(b), showing the exciton degradation of PL bands (365 ± 5 and 370 ± 5 nm). Our experimental results on the

degradation of the Si–Si chain and DB creation by radiation of 266 and 355 nm are in accord with the previous observations [27]. In PMPSi (figure 2) the silicon chain is attacked and DBs are formed by 266 nm photons in the place of absorption basically non-selectively, so that in the absorption in the σ–σ^* excitation of the Si–Si chain range no blue shift is observed [27]. On the other hand, radiation of 355 nm creates in PMPSi (figure 1(b)) an exciton of lower energy and the transport of the exciton to the longer segments of lower energy is observed, cutting them predominantly at the defects and WB in the Si–Si chain [26, 27]. This fact is manifested in the blue shift of the absorption with the progressive degradation process. In PBMSi the degradation of the Si–Si chain and DB creation by radiation of 266 and 355 nm is similar to that of PMPSi in the case of 355 nm radiation (figure 4(b)) and different for 266 nm radiation. From the comparison of the degradation kinetics of both examined materials it is obvious that there are basically two mechanisms operative, i.e. DB creation and DB reconstruction.

In our experiments, we concentrated on the creation of WBs during the degradation process. In figures 2(a) and 5(a) we compare the normalized PL spectra after 1 h degradation by radiation of 266 and 355 nm. We can observe the substantial increase in both then 400–420 nm and 500–600 nm bands after degradation. A similar PL band at 520–540 nm after photodegradation by 360 nm radiation was observed and was absent if 250–280 nm radiation was used [26]. This was interpreted as the creation of the structural defects. Nakayama *et al* [21] observed the growth of the PL band at 520 nm by degradation with radiation of 325 nm in a pre-photobleaching process in PMPSi.

We claim that the PL of the 500–600 nm band (and to some level the 400–420 nm band as well) is related to the WB formation at room temperature on the Si chain and exciton diffusion, free electron–hole formation, their trapping in WBs and their subsequent radiative recombination by tunnelling. Increase of the normalized PL 520–540 nm band can then be evaluated as the increase of the DOS of these WBs. The kinetics of WB creation is examined for PMPSi and PBMSi in figures 2(b) and 5(b). The efficiency of the WB creation in PMPSi (figure 2(b)) is greater for 266 nm radiation, supporting the idea of the suppressed exciton transport compared to the less energetical photon of 355 nm, where the WB creation is lowered due to the exciton migration to longer segments and/or already existing defects. For PBMSi (figure 5(b)) the WB creation kinematics for 355 nm degradation is similar to that of PMPSi in figure 2(b). The 266 nm degradation results then support the model calculations of DB and WB reconstruction in the more rigid Si skeleton [39].

The WBs in the glassy materials PMPSi and PBMSi exhibit metastability. This is visible in figures 3 and 6. The metastability issue was addressed in [13, 14] and [40] using transient photoconductivity and post-transit photoconductivity in PMPSi. We found [13] that the bond cleavage or weakening resulted in the formation of deep electronic states of differing parameters (energy positions and capture cross-sections). The WBs constitute deep electronic states situated 0.45–0.55 eV above the HOMO level depending on the energy of the excitation [13]. Kadashchuk *et al* [25] found metastability of the UV degradation induced peak situated at 0.45 eV after degradation by 250–280 nm and 366 nm radiation. These states are amenable to annealing with the activation energy of 0.65 eV. The existence of radiation-driven metastability and thermally driven recovery of Si–Si bonds was proved by the method of thermally stimulated luminescence.

The main conclusions may be formulated as follows.

(1) The WBs of polysilanes are formed as intrinsic defects that are deviations from the optimally bonded network and conformation.

(2) The PL of the 500–600 nm band is connected with the WBs on the Si chain—the exciton diffusion is followed by free electron–hole formation, trapping in WBs and radiative

recombination by tunnelling. Increase of the normalized PL 520–540 nm band after UV degradation can be then evaluated as the increase of the DOS of WBs.

(3) The efficiency of the WB creation in PMPSi is greater for 266 nm, supporting the idea of the limited exciton transport compared to the less energetical photon of 355 nm, where the WB creation is lowered due to the exciton migration to longer segments and/or already existing defects. For PBMSi the WB creation kinetics for 355 nm degradation is similar to that of PMPSi, whereas the 266 nm degradation results supports the model calculations of DB and WB reconstruction in the more rigid Si skeleton.

(4) The WBs exert metastability and increase disorder.

(5) The observed phenomena may contribute to the optimization of polysilane photo and electron resists.

Acknowledgments

The UV degradation experiments were done in the laboratory of Department of Physics at Trinity College in Dublin, Ireland; Professor W Blau and Dr Stephen Lipson are acknowledged for their support and help.

The authors are also indebted to the Grant Agency of the Academy of Sciences No. A100100622, and Ministry of Education, Youth and Sports of the Czech Republic for the support of this work in Czech–Chinese cooperation projects No. 1P05ME729 and 1P05ME734. The authors are also grateful to the Ministry of Education, Czech Republic, for providing financial support to carry out this research (Grant No. MSM 7088352101).

References

[1] Hayase S 1994 *Chemtech* **24** 19
[2] Fujiki A, Yoshimoto K, Yoshida M, Ohmori Y and Yoshino K 1995 *Japan. J. Appl. Phys.* **34** 1365
[3] Lacave-Goffin B, Demoustier-Champagne S and Devaux J 1999 *ACH-Models Chem.* **136** 215
[4] Shuzi H 2003 *Prog. Polym. Sci.* **28** 359
[5] Zallen R 1983 *The Physics of Amorphous Solids* (New York: Wiley)
[6] Navratil K, Sik J, Humlicek J and Nespurek S 1999 *Opt. Mater.* **12** 105
[7] Harrah L A and Zeigler J M 1987 *Macromolecules* **20** 601
[8] Ito O, Yoshimoto K, Yoshida M, Ohmori Y and Yoshino H 1995 *Japan. J. Appl. Phys.* **34** 1365
[9] Takeda K, Fujino M, Seki K and Inokuchi J 1987 *Phys. Rev.* B **36** 8129
[10] Mintmire J W and Ortiz J V 1988 *Macromolecules* **21** 1189
[11] Takeda K, Teramae H and Matsumoto N 1986 *J. Am. Chem. Soc.* **108** 8186
[12] Takeda K, Shiraishi K, Fujiki M, Kondo M and Morigaki K 1994 *Phys. Rev.* B **50** 5171
[13] Schauer F, Handlíř R and Nešpůrek S 1997 *Adv. Mater. Opt. Electron.* **7** 61
[14] Schauer F 1999 *Czech. J. Phys.* **49** 871
[15] Sawodny M, Stumpe J and Knoll W 1991 *J. Appl. Phys.* **69** 1927
[16] Street R A 1991 *Hydrogenated Amorphous Silicon* (Cambridge: Cambridge University) p 169
[17] Tanaka Ke 1990 *Rev. Solid State Sci.* **4** 511
[18] Naito H 2002 *Japan. J. Appl. Phys.* **41** 5523
[19] Schauer F, Dokoupil N, Horváth P, Kuřitka I, Nešpůrek S and Pospíšil J 2004 *Macromol. Symp.* **212** 563
[20] Allan G, Delerue C and Lannoo M 1993 *Phys. Rev.* B **48** 7951
[21] Nakayama Y, Kurando T, Hayashi H, Oka K and Dohmaru T 1996 *J. Non-Cryst. Solids* **198** 657
[22] Fujiki M 1992 *Chem. Phys. Lett.* **198** 177
[23] Nakayama Y, Inagi H and Zhang M 1999 *J. Appl. Phys.* **86** 768
[24] Naito H, Kodama S-I, Kang Q Z and Okuda M 1996 *J. Non-Cryst. Solids* **198–200** 653
[25] Kadashchuk A, Nešpůrek S, Ostapenko N, Skryshevskii Yu and Zaika V 2001 *Mol. Cryst. Liq. Cryst.* **355** 413
[26] Kadashchuk A, Ostapenko N, Zaika V and Nešpůrek S 1998 *Chem. Phys.* **234** 285
[27] Skryshevski Yu, Ostapenko N, Kadasshchuk A, Vakhnin A and Suto S 2001 *Mol. Cryst. Liq. Cryst.* **361** 37
[28] Ostapenko N, Telbiz G, Ilyin V, Suto S and Watanabe A 2004 *Chem. Phys. Lett.* **383** 456

[29] Schauer F, Kuritka I and Nespurek S 2004 *Polym. Degrad. Stabil.* **84** 383
[30] Nešpůrek S, Schauer F and Kadashchuk A 2001 *Mon. Chem.* **132** 159
[31] Miller D R and Michl J 1989 *Chem. Rev.* **89** 1359
[32] Ito O, Terajima M, Azumi T, Matsumoto N, Takeda K and Fujino M 1989 *Macromlecules* **22** 1718
[33] Wilson W L and Weideman T W 1991 *J. Phys. Chem.* **95** 4568
[34] Kanemitsu Y and Suzuki K 1995 *Phys. Rev.* B **5** 13103
[35] Watanabe A, Nanyo M, Sunaga T and Sekiguchi A 2001 *J. Phys. Chem.* A **105** 6436
[36] Toyoda S and Fujiki M 2001 *Macromolecules* **34** 2630
[37] Watanabe A, Miike H, Tsutsumi Y and Matsuda M 1993 *Macromolecules* **26** 2111
[38] Trommsdorf H P, Zeigler J M and Hochstrasser R M 1989 *Chem. Phys. Lett.* **154** 463
[39] Schauer F, Kuritka I and Nespurek S 2003 *ECME: Proc. 7th European Conf. on Molecular Electronics (Avignon, Sept. 2003)*
[40] Naito H, Zhang S and Okuda M 1994 *J. Appl. Phys.* **76** 3612